ISSN: 0067-2904

Study of Corrosion Inhibition for Some New Schiff Bases Synthesized from Quinazolinone Derivative

Aseel Jassim Mohammed*, Oday H. R. Al-Jeilawi
Department of Chemistry, College of Sciences, University of Baghdad, Baghdad, Iraq

Received: 18/6/2023 Accepted: 23/10/2023 Published: 30/12/2024

Abstract

In this work, new Schiff bases of quinazolinone derivatives (Q1-Q5) were synthesized from methyl anthranilate. The synthesis involved three steps. In the first step, methyl anthranilate was reacted with isothiocyanatobenzene, producing the thiourea derivative K1. The second step entailed reacting K1 with hydrazine hydrate, synthesizing 3-amino-2-(phenylamino) quinazolin-4(3H)-one (K2). The third step involved reaction of K2 with various aromatic aldehydes, yielding the Schiff bases derivatives Q1-Q5. The chemical structures of these compounds were identified by FT-IR, ^{1}H NMR and ^{13}C NMR spectroscopy. The newly synthesized derivatives (Q1-Q5) were subjected to rigorous evaluation to assess their efficacy as corrosion inhibitors for carbon steel in an acidic environment (1M HCl). Weight loss measurements were employed, and the concentration of the compounds was varied to gauge their performance at ambient temperature. Among the array of compounds tested, Q1 exhibited remarkable performance, particularly when employed at a concentration of 0.5 M. The corrosion inhibition properties of compound Q1 were evaluated. It exhibited excellent inhibition efficiency, reaching a peak of 93% according to the investigation. Further dynamic polarization analysis revealed some interesting relationships between inhibition efficiency, concentration, and temperature. Specifically, higher concentrations and lower temperatures led to enhanced inhibition by Q1.

Keywords: corrosion inhibitors, quinazolinone derivatives, Schiff bases, weight loss, polarization

دراسة تثبيط التآكل لبعض قواعد شف الجديدة المحضرة من مشتق االكوينازولينون

اسيل جاسم محمد , عدي هادي رؤوف الجيلاوي
قسم الكيمياء, كلية العلوم , جامعة بغداد , بغداد , العراق

الخلاصة

في هذا العمل تم تحضير قواعد شف جديدة لمشتق الكوينازولينون (Q1–Q5) من انثرانيلات المثيل. التحضير تضمن ثلاث خطوات. في الخطوة الاولى، تم تفاعل انثرانيلات المثيل مع إيزوثايوسيانات البنزين لينتج مشتق ثايويوريا (K1). في الخطوة الثانية تم مفاعلة (K1) ع الهيدرازين المائي لتحضير 3–امينو–2–(فنيل امينو) كوينازولين–4(3H)–اون (K2). الخطوة الثالثة تضمنت تفاعل (K2) مع الديهايدات اروماتية متنوعة للحصول على مشتقات قواعد شف (Q1–Q5). التركيب الكيميابي في هذه المركبات تم تشخيصه باستخدام تقنيات التحليل الطيفي بما في ذلك التحليل الطيفي للاشعة تحت الحمراء والرنين النووي المغناطيسي للبروتون

*Email: Aseel.jasim1205m@sc.uobaghdad.edu.iq

والكاربون (13). بعد ذلك خضعت المشتقات الجديدة المحضرة (Q1–Q5) لتقييم فعاليتها كمثبطات لتآكل الصلب الكربوني في بيئة حامض الهيروكلوريك (1 مولاري). باستخدام قياسات فقدان الوزن بتراكيز مختلفة في درجة حرارة الغرفة، وكان أفضلها Q1 في وجود 0.5 مولاري. تم تقييم خواص تثبيط التآكل للمركب Q1. أظهر كفاءة تثبيط رائعة، حيث وصل إلى قمة 93٪ وفقًا للتحقيق. كشف التحليل الديناميكي للاستقطاب عن بعض العلاقات المثيرة للاهتمام بين كفاءة التثبيط والتركيز ودرجة الحرارة. على وجه التحديد، أدت مستويات التركيز الأعلى ودرجات الحرارة الأقل إلى تعزيز تثبيط Q1.

1. Introduction

Carbon steel, a widely utilized material in chemical and petroleum industries [1], boasts affordability and a robust mechanical structure [2]. However, its vulnerability to corrosion poses significant challenges in various environmental conditions. Factors such as equipment descaling, acidic solution cleaning, acidification of crude oil wells, acid pickling, and etching contribute to the corrosion of iron alloys [3]. Such reactions, transitioning from metallic to ionic states, can result in substantial financial losses [4]. To counter these issues, effective corrosion control techniques are urgently needed. Multiple approaches exist to prevent rust, including paint cathodic protection, proper material selection during construction, and the utilization of corrosion inhibitors [5]. The application of corrosion inhibitors has proven to be a practical and potent strategy [6]. Extensive research has highlighted the efficacy of corrosion inhibitors in mitigating the corrosion of mild steel. These chemical substances, when added in minute quantities to a metal surface or corrosive environment, significantly reduce metal corrosion [7]. Organic compounds with heteroatoms like nitrogen, oxygen, and sulfur exhibit exceptional corrosion inhibition properties. Their high polarizability and low electronegativity enable them to cover large metallic surfaces and efficiently transfer electrons to unoccupied orbitals, enhancing their effectiveness as inhibitors [8]. Typically, the corrosion products comprise small quantities of metals and metal oxides [9, 10]. The relentless accumulation of corrosion products over time inflicts detrimental consequences on the optimal functioning of boilers [11]. A plethora of scientific inquiries have delved into the realm of employing organic compounds as formidable guardians against mild steel corrosion within diverse acidic solutions, with a profound emphasis on the intricate interplay between metal surfaces and heteroatoms, encompassing the likes of nitrogen, oxygen, and sulfur. These remarkable heteroatoms, housing an abundant supply of free electron pairs, assume an indispensable role in thwarting the relentless onslaught of corrosion [12]. Notably, compounds with p-bonds demonstrate remarkable inhibition capabilities, leveraging the prowess of their p-orbitals to facilitate an electron transfer extravaganza [13]. The enduring influence of thiourea and its derivatives as corrosion inhibitors on carbon steel surfaces immersed in acidic media is a testament to their unrivaled corrosion-preventing prowess [14]. Among the vast array of corrosion inhibitors, the esteemed Schiff base azomethine molecules, brimming with their distinctive (C=N) group, emerge as stalwart defenders against the perils of corrosion [15]. A meticulous review of the scientific literature underscores the resounding efficacy of organic inhibitors housing both sulfur and nitrogen moieties in the enduring battle against steel corrosion in an acid-laden landscape, encompassing monomeric acids such as the potent hydrochloric acid and its formidable counterpart sulfuric acid [16]. Extensive prior investigations into the realm of corrosion inhibitors have bestowed profound attention upon the synthesis of quinazolinone derivatives, unfurling their potential as stalwart guardians of steel alloys [17]. Pioneering research ventures have irrefutably established the prowess of Schiff bases in curbing the insidious oxidation of mild steel, copper, zinc, and aluminum when confronted with their malevolent adversaries lurking within hostile solutions [18]. In this study, we synthesized new Schiff bases (Q1-Q6) and thoroughly evaluated their effectiveness as corrosion inhibitors for carbon steel in an acidic environment (1M HCL).

2. Experimental

2.1 Materials and Methods

All chemicals and solvents used in this work are from Fluke, BDH companies. Melting points of the compounds were determined using a Gallenkamp capillary melting point apparatus with open glass capillaries. The melting points measured were uncorrected. Infrared spectral data was collected using a Shimadzu 8400 Fourier Transform Infrared (FT-IR) spectrometer. This allowed for characterization of functional groups present in each compound via analysis of peak absorption wavelengths. A Bruker Vance 400 MHz spectrometer was used to record the ^{1}H NMR and ^{13}C NMR spectral data. Using DMSO-d_6 as a reference and tetramethylsilane (TMS) as the internal standard, chemical shifts are reported in ppm downfield. Corrosion measurement by using (EmStat 4s, Palm Sens, Holland) . TLC sheets (silica gel-covered aluminum sheets) were utilized to monitor the reactions, and the eluent was utilized as a combination of hexane and ethyl acetate and visualized using iodine**.**

2.2 Synthesis of Inhibitors

2.2.1 Synthesis of Methyl-2-(3-phenylthioureido)benzoate (K1) [19]

The reaction was initiated by dissolving 1.3 ml (0.001 mol) of methyl anthranilate in 5 ml of absolute ethanol. To this solution, 1.2 ml (0.001 mol) of isothiocyanatobenzene was added. The reaction mixture was refluxed for 15 hours, the reaction is monitored by TLC , a solvent system hexane: ethyl acetate (3:2).The solution was added to crushed ice then filtered the precipitate, washed in ethanol and water and left to dry. The physical characteristics of the compound K1 obtained is listed in Table 2.

2.2.2 Synthesis of 3-Amino-2-(phenylamino) quinazolin-4(3H)-one (K2) [19]

Methyl-2-(3-phenylthioureido) benzoate (K1) (0.5 g, 0.001 mol) was dissolved in 6 mL of dimethylformamide (DMF) and heated until K1 completely dissolved. Initially, the solution had a brown color. Excess hydrazine hydrate (4 mL) was added, resulting in a color change to turquoise. the reaction completion after refluxed for 8 hours based on TLC, a solvent system hexane: ethyl acetate (3:2). then the mixture was added to crushed ice. The final product was filtered, washed with water and left to dry. The physical characteristics of the compound K2 obtained is listed in Table 2.

2.2.3 Synthesis of inhibitors 3-[(E))-[(substituted phenyl)methylidene]amino]-2-(phenyl amino)-3,4-dihydroquinazolin-4-one(Q1-Q5) [20]

The reaction mixture was prepared by dissolving 0.001 moles of the aromatic aldehyde in 10 mL of ethanol. A few drops of glacial acetic acid were also added to the solution. Then, 0.001 moles of K2 were added to this solution containing the aromatic aldehyde in ethanol/acetic acid. The reaction mixture was refluxed for 7-9 hours. The reaction was monitored by TLC (hexane/ ethyl acetate, 3:2). then the mixture was added to crushed ice The precipitate was then filtered, washed with water and dried, the physical characteristics of the synthesized compounds are provided in Table (2).

2.3 Preparation of Specimens

The construction of the artificial electrode for carbon steel 45 involved meticulous preparations. The chemical composition (wt %) of the electrode, as detailed in Table 1, provided crucial insights. The electrodes employed in each experimental trial were precisely cut into dimensions of 2*2*0.1 (cm), ensuring uniformity and accuracy. To ensure the optimal surface quality, a multi-step approach was employed. It commenced with a systematic progression through a series of emery paper grades, consisting of eight papers. These papers, with varying grit sizes ranging from No. 150 to No. 2000, were employed to achieve the desired surface texture and smoothness. This diverse range of grit sizes offered a spectrum of

abrasiveness, facilitating the meticulous preparation of the electrode surface. Following the emery paper treatment, the electrodes underwent a rigorous cleansing process. The electrodes underwent a meticulous cleaning process involving two rounds of washing with acetone to effectively eliminate any dirt or impurities that might compromise the precision of the experiments. The second process contains using double distilled water, to ensure the complete removal of any residual traces of acetone or other solvents.

Table 1: The chemical composition of carbon steel 45

Metal	C%	SI%	Mn%	S%	P%	Cu	Ni%	Cr%	Fe%
Carbon Steel 45	0.36-0.42	0.15-0.30	1.00-1.40	0.05	0.05	0.50	0.20	0.20	96.88-97.49

2.4 Preparation of Solutions

2.4.1 preparation of Blank solution

To prepare a 1M solution of hydrochloric acid (HCl), 85.9 ml of concentrated HCl (36% w/w, density = 1.18 g/ml) was measured and added to a 1000 ml volumetric flask. This flask was then filled to the mark with distilled water to achieve the final volume. This process resulted in a 1M HCl solution through dilution of the concentrated acid stock with water in the volumetric flask.

2.4.2 preparation of inhibitor Solutions

The solutions concentration of [0.01, 0.05, 0.1 and 0.5] M were prepared by dissolving synthesized Schiff bases (Q1-Q5) in (1M HCL).

2.5 weight loss measurement

The experimentation phase commenced with the meticulous weighing of carbon steel samples using a precise electronic balance. These samples were then immersed in separate beakers containing 1 M HCL solution. After precisely 1 hour at a controlled temperature of 293K, the specimens were delicately extracted from the corrosive environment. Subsequently, a comprehensive cleansing process was employed, involving suspension and complete immersion of the samples in 250 ml of water to ensure the elimination of any residual corrosion products. Thorough washing with acetone followed suit. Finally, the samples underwent careful drying in an oven, after which their weights were once again measured. The weight loss measurements adhered to the well-established ASTM system [21,22]. Rigorous repetition of the experiments was undertaken to verify the reliability of the findings, taking into account the standard deviation of the weight reduction. With these data, the average corrosion rate in milligrams per square centimeter per hour could be calculated, employing the formula (1) specifically designed for the corrosion rate determination of mild steel [23].

$$W=\Delta M/S*t \quad \text{---------} \quad (1)$$

ΔM = mass loss (in grams) , S = area (in square meters) , t = immersion time (hours)
Using an equation (2), we were able to calculate the percentage of inhibition efficiency.
(IE %)= percentage inhibition efficiency [24]:

$$IE\% = ((W - W_{inh}) / W) \times 100 \quad \text{--------} \quad (2)$$

W= the mild steel corrosion rates in absence of an inhibitor
W (inh)= the mild steel corrosion rates in the presence of an inhibitor.

3. Results and discussion

3.1. Chemistry

To develop new Schiff bases derivatives (Q1-Q5) as corrosion inhibitors, we synthesized organic compounds containing nitrogen (N) and sulfur (S) atoms. Scheme (1), illustrates the synthesis process, where compound K1 was prepared following established procedures [19]. The scheme involved reacting methyl anthranilate with isothiocyanateobenzene to produce thiourea derivative (K1), The FT-IR spectral data of compound (K1) showed the disappearance absorbance of υ (NH_2) for methyl anthranilate while appearance a new two absorption at (3245) cm^{-1}, which was attributed to the secondary amine group υ (NH), in addition stretching and bending vibrations at (1533, 1288 and 989) cm^{-1} due to involving interaction between (C=S) group and (C-N) group of the C=S group attached to a nitrogen atom [25,26]. These bands which are good evidence for the formation of the compound (K1). Compound (K2) prepare from reaction of K1 with excess hydrazine hydrate. FT-IR spectral data showed the disappearance of υ (C=S), while appearance a new two stretching vibrations at (3450) and (3305) cm^{-1} for (NH_2) and bands at (1660) cm^{-1} (1616) cm^{-1} due to C=O amide and C=N respectively. The ^{1}H NMR spectral data of compound K2 showed singlet signal at 5.8 ppm, which belong to the NH_2 proton and singlet signal at 9.8 ppm, which belong to the N-H proton [27]. In the final step, Schiff bases derivatives (Q1-Q5) were prepared by reacting K2 with various aromatic aldehydes in an acidic medium. The progress of the reaction was monitored using Thin-Layer Chromatography (TLC) for all derivatives. The FT-IR spectral data of compounds (Q1-Q5) showed new stretching vibrations ranging from (1612-1620) cm^{-1} attributed to the C=N bond of the azomethine group overlap with C=N quinazoline ring [27] and disappearance stretching vibrations of (NH_2). All details of the FT-IR spectral data for the prepared compounds K1, K2 and (Q1-Q5) are listed in Table 2. The ^{1}H NMR spectral data of compounds (Q1-Q5) showed singlet signals at 8.98-11.6 ppm, which belong to the N-H proton, 6.77-8.26 ppm for aromatic protons and normal range of the chemical shifts at 7.96-9.5 ppm due to azomethine proton (C<u>H</u>=N). The ^{13}C NMR spectral data of compounds (Q1-Q5) showed signals at 140.06-167.46 ppm, which belong to the azomethine carbon (<u>C</u>H=N). The protons of the amino group in compound K2 did not appear in the ^{1}H NMR spectra of derivatives (Q1-Q5) and appearance new peak for carbon (azomethine group) in the ^{13}C NMR spectra which could be good evidence to formation of Schiff bases. ^{1}H NMR and ^{13}C NMR spectral data for the prepared compounds K2 and (Q1-Q5) are listed in Table 3 and Table 4 respectively.

Table 2: The physical characteristics and FT-IR spectral data of the synthesized compounds

Code	Molecular formula	M.W. (g/mol)	Color	M.P.^{oC}	Reflux time hrs.	Yield %	FT-IR (υ, cm^{-1})
K	$C_8H_9NO_2$	151.16	Colorless liquid	24	/	/	3481 (asym) ,3373 sym (NH_2) 1693(C=O) ester
K1	$C_{15}H_{14}O_2N_2S$	286.35	white	314-316	15	54.5	3245(N-H) 3029 (C-H $_{aroma}$),2968,2891(C-H $_{aliph}$), 1662(C=O)ester, 1533,1289,989(C=S) interaction with (N-C=S)
K2	$C_{14}H_{12}ON_4$	252.28	brown	164-162	8	86.3	3450(NH_2) asym, 3305(NH_2) sym 3224(N-H),3058(C-H $_{aroma.}$), 1660(C=O),1616(C=N), 1577(C=C$_{arom.}$)
Q1	$C_{21}H_{15}O_3N_5$	385.38	yellow	256-258	7	86.8	3188(N-H),3082(C-H $_{aroma.}$),2960,2852(C-H

							$_{aliph.}$),1679(C=O), 1612(C=N $_{quinazoline\ ring}$ overlap with CH=N $_{(azomethine)}$),1577(C=C $_{arom.}$), 1519,1342(NO_2,asym, sym)
Q2	$C_{21}H_{16}O_2N_4$	356.38	white	290-293	7	35.7	3247(O-H),3136(N-H), 3070(C-H $_{arom.}$) 2958,2852(C-H $_{aliph.}$), 1662 (C=O), 1620 (C=N $_{quinazoline\ ring}$ overlap with CH=N $_{(azomethine)}$), 1531(C=$C_{arom.}$)
Q3	$C_{21}H_{15}O_3N_5$	385.38	Dark yellow	174-177	9	65.7	3220(N-H),3070(C-H $_{aroma.}$),2972,2854(C-H aliph),1670(C=O), 1620(C=N $_{quinazoline\ ring}$ overlap with CH=N $_{(azomethine)}$),1573(C=C) 1523,1342(NO_2 asym and sym).
Q4	$C_{23}H_{21}ON_5$	383.45	Dark orange	286-288	8	64.4	3224(N-H),3134(C-H $_{aroma.}$),2964,2821(C-H $_{alliph.}$)1662(C=O), 1620((C=N $_{quinazoline\ ring}$ overlap with CH=N $_{(azomethine)}$),1593(C=C $_{arom.}$).
Q5	$C_{22}H_{18}O_2N_4$	370.41	brown	296-298	9	54.79	3217(N-H), 3072(C-H $_{arom.}$), 2962,2839(C-H $_{aliph.}$), 1662(C=O), 1620(C=N $_{quinazoline\ ring}$ overlap with CH=$N_{(azomethine)}$),1577(C=$C_{aroma.}$).

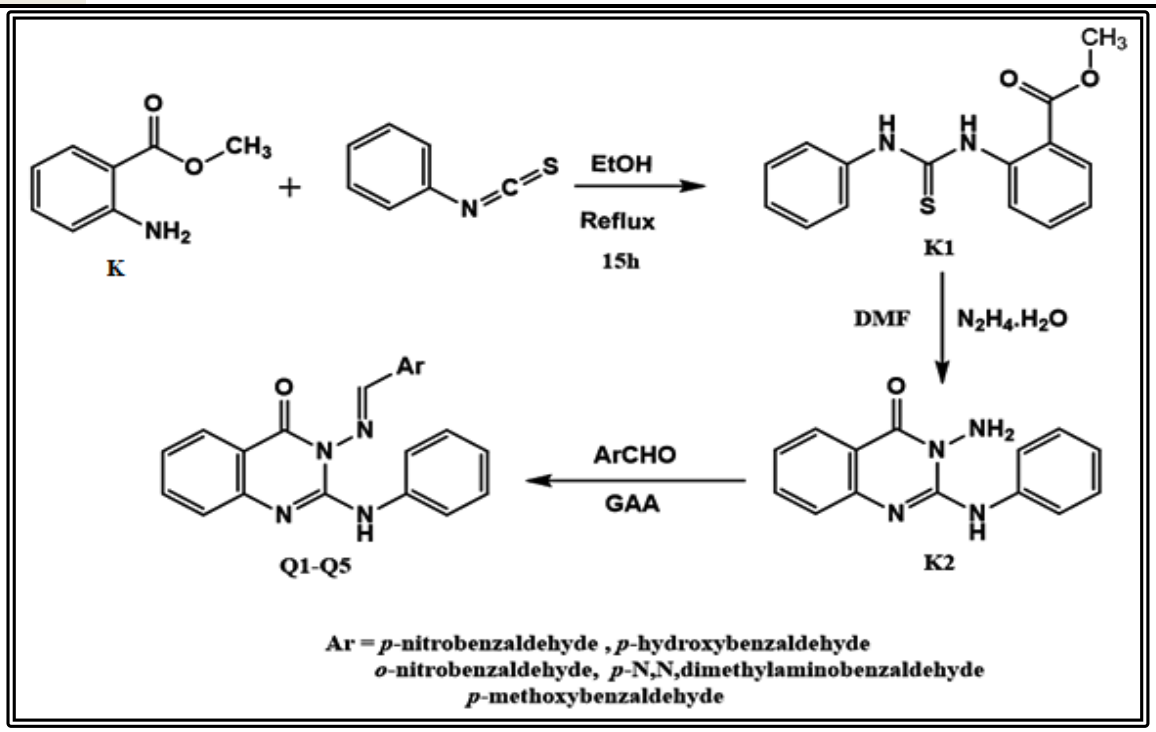

Scheme 1: Schiff bases synthesized from quinazolinone derivative

Table 3: Data of ^{1}HNMR spectrum (ppm) for synthesized compounds

Comp. No.	Compound structure	^{1}HNMR parameters (ppm)
K2	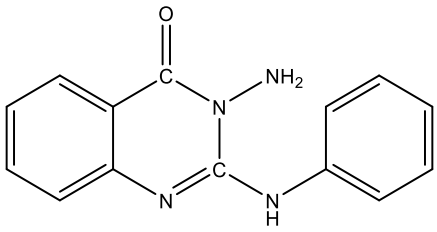	5.8(s,2H,N<u>H₂</u>) 7.03-8.91(m,9H,Ar-**<u>H</u>**) 9.8 (s,1H,N<u>H</u>)
Q1	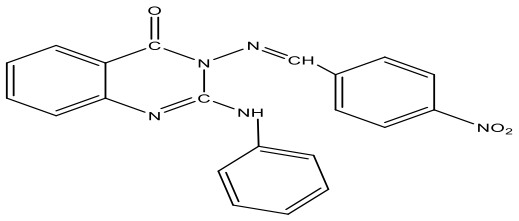	7.35-8.26(m,13H,Ar-**<u>H</u>**) 8.29 (s,1H,-C**<u>H</u>=N**) 9.67(s,1H,-N**<u>H</u>)**
Q2	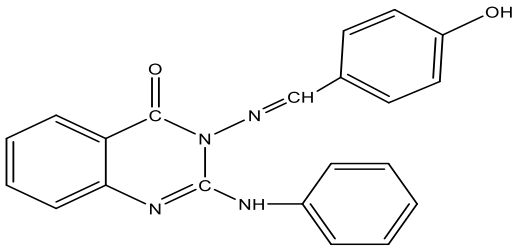	6.85-8.22 (m,13H,Ar-**<u>H</u>**) 8.5(s,1H,-C**<u>H</u>**=N) 10.11(s,1H,N**<u>H</u>**) 13.07(s,1H,O**<u>H</u>**)
Q3	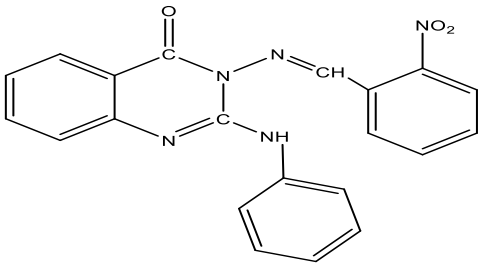	6.85-8.22(m,13H,Ar-**<u>H)</u>** 8.56(s,1H, -C<u>H</u>=**N)** 8.98(s,1H,N**<u>H</u>**)
Q4	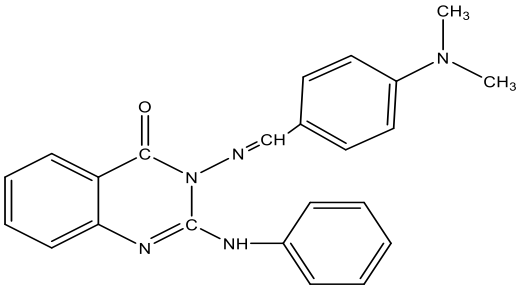	3.04(S,6H,N-C**<u>H₃</u>**) 6.77-7.79(m,13H,Ar-**<u>H</u>**) 7.96(S,1H,-C**<u>H</u>**=N) 9.70(S,1H,N**<u>H</u>**)
Q5	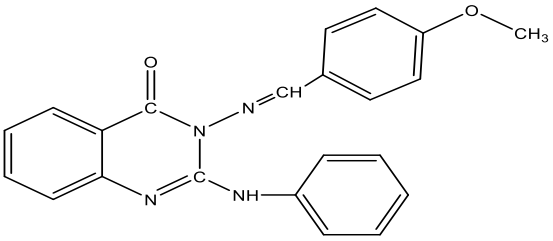	3.89(s,3H,O-C**<u>H₃</u>**) 7.12-8.26(m,13H,Ar-**<u>H</u>**) 9.56(s,1H,-C**<u>H</u>**=N) 9.87(s,1H,N**<u>H</u>**)

Table 4: Data of ^{13}CNMR spectrum (ppm) for synthesized compounds

Comp. No.	Compound structure	^{13}CNMR data (ppm)
K2	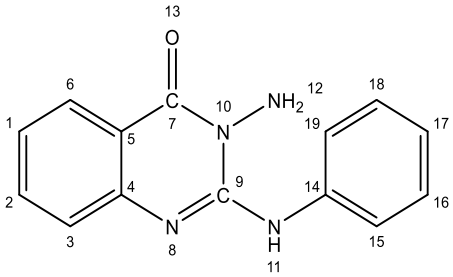	116.17-162.6(C_1-C_6 and C_{14}-C_{19}), 167.32(C_9),176.50(C_7).
Q1	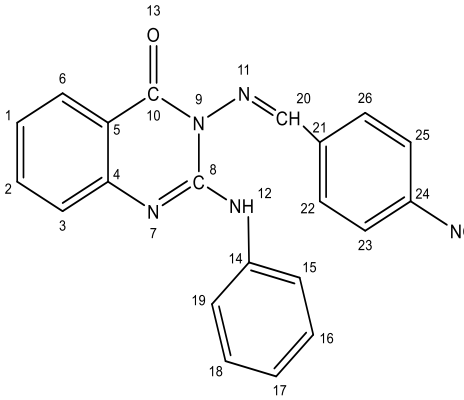	124.50-143.56(C_1-C_6, C_{14}-C_{19}, C_{21}-C_{23}, C_{25} and C_{26}), 148.01(C_{24}), 148.17(C_8), 166.52 (C_{20}), 172.87 (C_{10}).
Q2	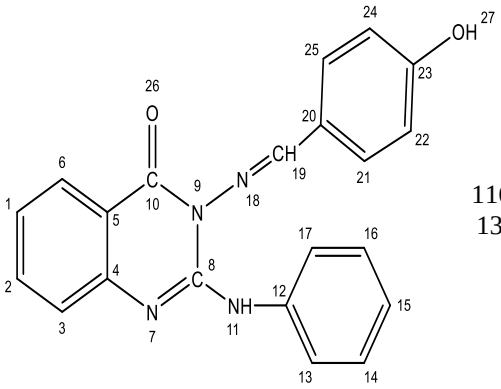	116.16-136.09(C_1-C_6, C_{12}-C_{17}, C_{20}-C_{22}, C_{24} and C_{25}), 139.78(C_8), 140.06(C_{19}), 160.29(C_{23}), 176.52(C_{10}).
Q3	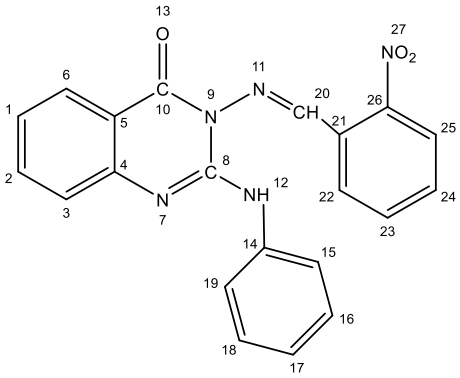	122.37-149.35(C_1-C_6, C_{14}-C_{19} and C_{21}-C_{25}), 153.03(C_{20}), 159.26(C_{26}), 161.08(C_8), 176.52(C_{10}).

Q4	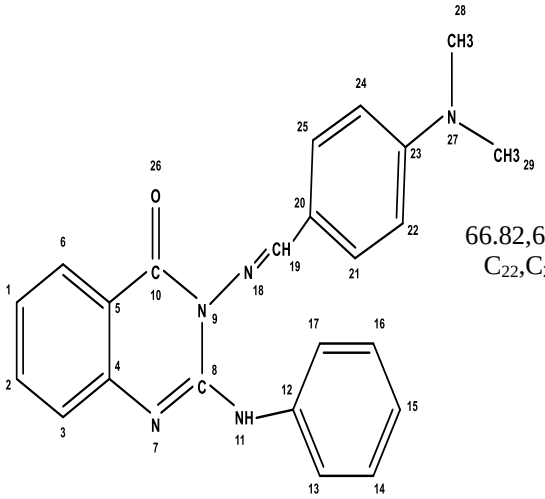	66.82,67.85(C_{28},C_{29}),111.5-140.06(C_1-C_6, C_{12}-C_{17}, C_{20}-C_{22},C_{24} and C_{25}), 154.64(C_8), 160.28(C_{23}), 167.46 (C_{19}), 176.52(C_{10}).
Q5	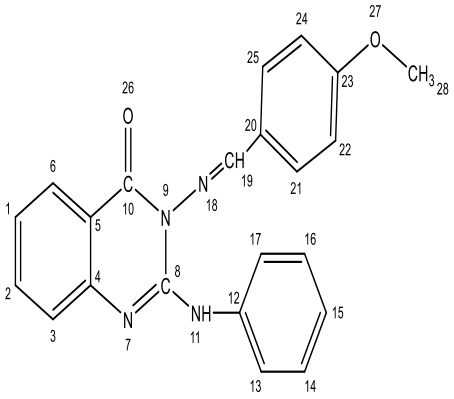	56.17(C_{28}), 114.98-140.06(C_1-C_6, C_{12}-C_{17}, C_{20}-C_{22}, C_{24} and C_{25}), 148.98(C_8), 160.29(C_{19}), 164.68(C_{23}). 176.52(C_{10}),

3.2 The measures of weight loss

Gravimetric measurements were carried out on carbon steel samples under two corrosion conditions involving 1M HCl solution: without inhibitors (control) and with various Schiff base inhibitors. Specifically, the inhibitors tested were quinazolinone derivatives Q1 through Q5. By weighing the carbon steel specimens before and after immersion, the corrosion rates in 1M HCl could be compared in the absence and presence of these Schiff base inhibitors derived from quinazolinone. The immersion duration was one hour at a temperature of 293K. We analyzed and identified the corrosion rate and inhibition effectiveness of the inhibitors by measuring the weight loss of the samples. When testing the effectiveness of the (Q1-Q5) inhibitors at various concentrations (0.01M, 0.05M, 0.1M, and 0.5M), it was found that raising the inhibitor concentration led to a decrease in the rate of corrosion. In addition, an increase in inhibitor concentration was directly correlated with an increase in the efficiency of the inhibition. The results, including the corrosion rate and inhibition effectiveness for each recommended inhibitor (Q1-Q5), are presented in Table (5).

Table 5: corrosion rate and inhibition efficiency from measurements of weight loss for blank and inhibitors (Q1-Q5)

CODE	Conc.(M)	corrosion rate (C.R) $mg/cm^2.h$	surface coverage (Ɵ)	IE%
BLANK	/	/	/	/
Q1	0.01	0.25	0.747	74.74
	0.05	0.18	0.818	81.81
	0.1	0.099	0.9	90
	0.5	0.06	0.93	93
Q2	0.01	0.49	0.50	50
	0.05	0.45	0.54	54
	0.1	0.42	0.57	57
	0.5	0.40	0.59	59
Q3	0.01	0.27	0.727	72.7
	0.05	0.22	0.777	77.7
	0.1	0.19	0.80	80.8
	0.5	0.11	0.88	88.8
Q4	0.01	0.37	0.62	62.6
	0.05	0.33	0.666	66.6
	0.1	0.29	0.70	70
	0.5	0.25	0.74	74
Q5	0.01	0.595	0.595	59.5
	0.05	0.616	0.616	61.6
	0.1	0.666	0.666	66.66
	0.5	0.696	0.696	69.6

3.3 Study of potentiation polarization

Prior to the commencement of testing, the electrode potential was given a settling time of 15 minutes after adjusting its Tafel polarization. The electrode potential was modified to achieve this. Curves were automatically generated at a scan rate of 2.0 mV/s, ranging from -200 mV vs open circuit potential (OCP) to +200 mV vs OCP. The range of the curves was determined based on the open circuit potential. Each experiment was conducted at temperatures of 293 K, 303 K, 313 K, and 323 K. Calculations were made to determine the corrosion current density (Icorr) and the corrosion potential (Ecorr) in both the absence and presence of an inhibitor at concentrations of (0.01M, 0.05M, 0.1 M, and 0.5M). On a logarithmic scale, lines depicting potential versus Icorr were shown. [28-30]

3.4 Polarization measurements

Potentiostatic polarization curves were generated to examine the corrosion of carbon steel in a 1M HCL solution under different temperatures, both in the absence and presence of newly synthesized amino quinazolinone derivatives. Figure 1 illustrates the behavior of the solution at temperatures of 293 K, 303 K, 313 K, and 323 K with and without the inhibitor Q1 . The Tafel slope, which represents the linear relationship, was considered. By combining the samples tested in the anodic and cathodic potential domains, as discussed earlier, the controlled cathodic reaction was suppressed, leading to a reduction in current densities. These findings suggest that the studied inhibitors likely exhibit a mixed inhibition behavior. Notably, the corrosion potential remained unchanged when using these inhibitors, indicating inhibition of both the anodic and cathodic processes. Although there were slight variations in potentials due to the competition between these processes, the values of the electrochemical parameters are presented in Table 6 [31].

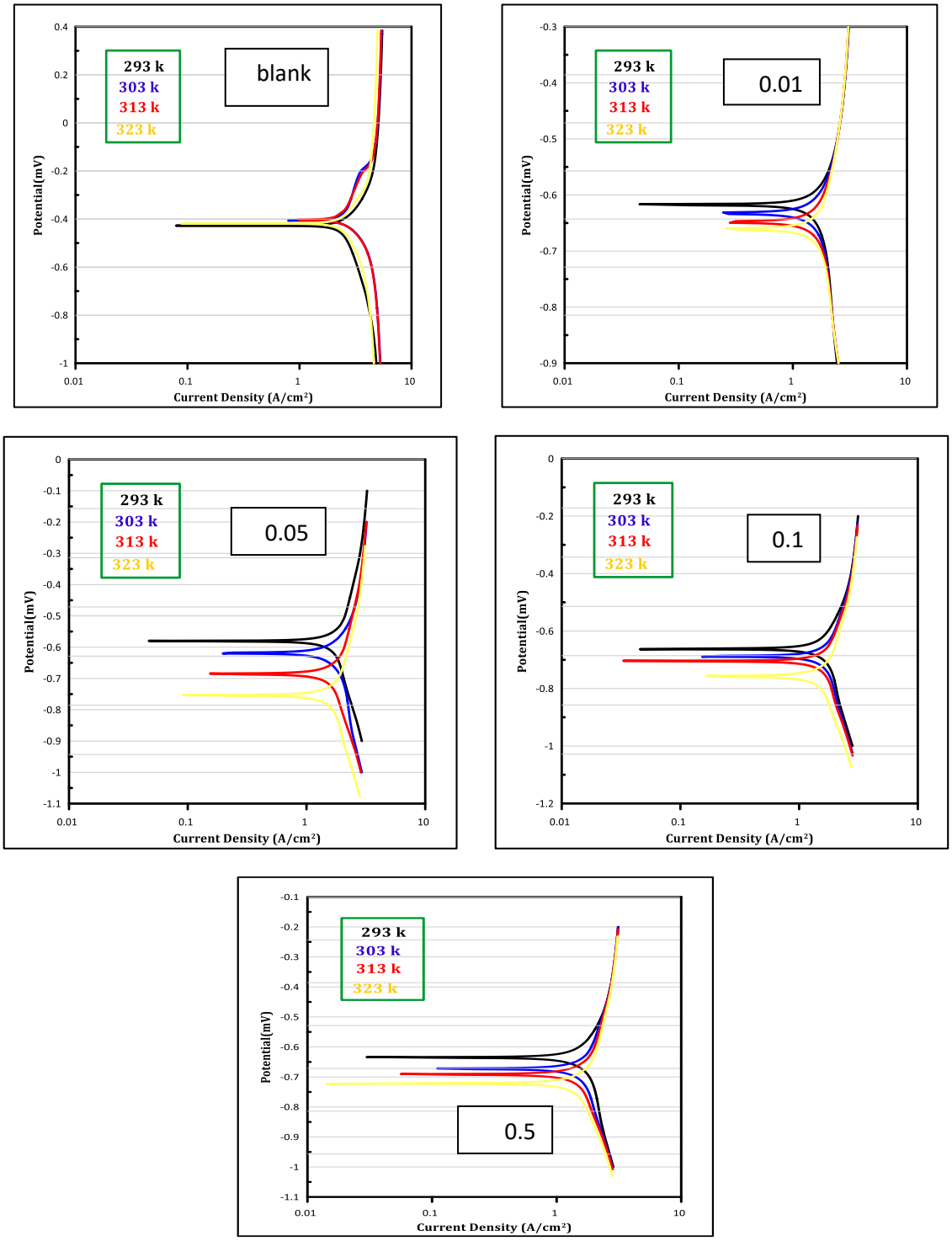

Figure 1: Polarization curves for corrosion of inhibitor Q1 solution in different temperature

Table 6: the corrosion parameters for both the blank and the compound Q1 in HCl solutions throughout a variety of concentration and temperatures.

Comp.	Temp.	E corr.	I corr.	I corr./ r	Resis.	Anodic β	Cathodic β	Corr. rate,	IE%
Blank	**293**	-0.430	228.9	2.489E-4	114.5	0.100	0.189	1.222	-
	303	-0.404	237.8	2.578E-4	89.47	0.192	0.073	1.265	-
	313	-0.382	255.1	2.751E-4	97.71	0.158	0.102	1.350	-
	323	-0.412	269.6	2.896E-4	101.4	0.113	0.168	1.421	-
0.01	**293**	-0.625	33.62	6.725E-5	1839	0.203	0.476	0.330	85
	303	-0.666	35.30	7.060E-5	1943	0.262	0.399	0.346	85
	313	-0.698	37.69	7.537E-5	1892	0.318	0.339	0.370	85
	323	-0.704	39.58	7.915E-5	1903	0.330	0.366	0.388	85
0.05	**293**	-0.739	24.82	4.965E-5	2327	0.321	0.227	0.244	89
	303	-0.715	26.09	5.219E-5	2473	0.309	0.287	0.256	89
	313	-0.618	29.33	5.867E-5	1780	0.187	0.338	0.288	89
	323	-0.727	31.93	6.387E-5	2240	0.349	0.312	0.313	88
0.1	**293**	-0.680	16.16	3.233E-5	2911	0.210	0.224	0.159	93
	303	-0.658	18.89	3.778E-5	2789	0.210	0.288	0.185	92
	313	-0.716	20.47	4.095E-5	2993	0.290	0.274	0.201	92
	323	-0.667	23.55	4.710E-5	2724	0.256	0.350	0.231	91
0.5	**293**	-0.633	8.183	1.637E-5	2889	0.104	0.114	0.080	96
	303	-0.671	11.46	2.293E-5	2923	0.135	0.180	0.113	95
	313	-0.688	13.96	2.791E-5	3126	0.170	0.246	0.137	95
	323	-0.725	16.51	3.302E-5	3007	0.251	0.210	0.162	94

E corrosion, V; I corrosion, μA; I corrosion per surface area, A/cm² ; Polarization Resistance, Ω ; Anodic β Tafel constant, V/decade ; Cathodic β Tafel constant, V/decade ; Corrosion rate, mm/year and IE% inhibition efficiency.

To calculate the percentage of inhibition efficiency (% IE) for the corrosion of carbon steel,

the following formula was used [32]:

$$\% IE = ((Icorr - Icorr_{inh}) / Icorr_{inh}) \times 100 \quad \text{--------- (3)}$$

$$\Theta = ((Icorr - Icorr_{inh}) / Icorr_{inh}) \quad \text{---------- (4)}$$

Icorr and Icorr $_{inh}$ are the corrosion current densities that are measured when organic inhibitors are not present and when they are present, respectively. These values were derived by extrapolating the cathodic and anodic Tafel lines to the corrosion potential, which is denoted by the symbol Ecorr; the % IE was calculated using equation 3. [33-35].

3.5 The effect of the inhibitor's concentration

The impact of Q1 inhibitor at different concentrations (0.01M, 0.05M, 0.1M, and 0.5M) was investigated. As indicated in Table (6), increasing the inhibitor concentration resulted in a reduction in the corrosion rate. Moreover, Figure (2) illustrates that higher inhibitor concentrations corresponded to increased inhibition effectiveness. These findings suggest that the inhibitor acts by obstructing the reaction sites on the surface of the carbon steel, preventing both the anodic and cathodic reactions. Notably, the inhibitor did not significantly alter the anodic and cathodic Tafel slopes, indicating its mixed-type inhibition behavior. The findings described above provide evidence supporting the conclusion that the investigated inhibitor displays adsorptive behavior [36].

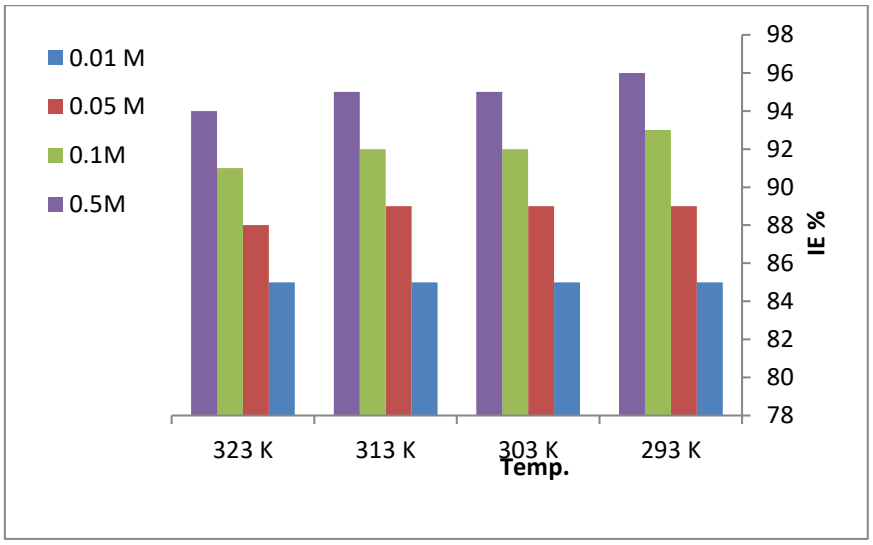

Figure 2: Relationship between inhibition efficiencies for inhibitor [Q1] with various concentrations and different temperature for carbon steel in HCL (1M).

3.6 Adsorption isotherms

Adsorption isotherms play a crucial role in understanding the interaction between inhibitors and metal surfaces. In this context, the substitutional adsorption process between organic molecules in the aqueous solution (Org(sol)) and water molecules previously adsorbed on the metal surface (H_2O (ads)) is a possible mechanism for the adsorption of organic adsorbates at the metal-solution interface [37].

$$Org\ (sol) + x\ H_2O\ (ads) = Org\ (ads) + xH_2O\ (sol) \quad \ldots\ldots\ldots\ (5)$$

where H2O (ads) is the water molecule adsorbed on the metallic surface, Org(sol), and Org(ads) are the organic species in the bulk solution and one on the metallic surface, respectively; x is the size ratio indicating the number of water molecules replaced by one organic adsorbate. In order to determine the adsorption isotherm, Equation 4 was used to compute the degree of surface coverage for a variety of inhibitor dosages that were dissolved in 1M HCL solution. Table (7) displays the values of the Θ. Following is an equation that, in line with Langmuir's isotherm, links the inhibitor concentration (C) to the surface coverage Θ. [38]:

$$\frac{C}{\theta} = \frac{1}{Kads} + C \quad \ldots\ldots\ldots\ (6)$$

Where Kads is the inhibitor adsorption process's equilibrium constant. Figure (3) illustrates the plot of C/ vs C, which results in a straight line. The coefficient of linear correlation. (r^2) is nearly equal to 1 and the slope is extremely close to 1, showing that the adsorption of

synthetic inhibitor (Q1) on the surface of carbon steel complies with the Langmuir adsorption isotherm.

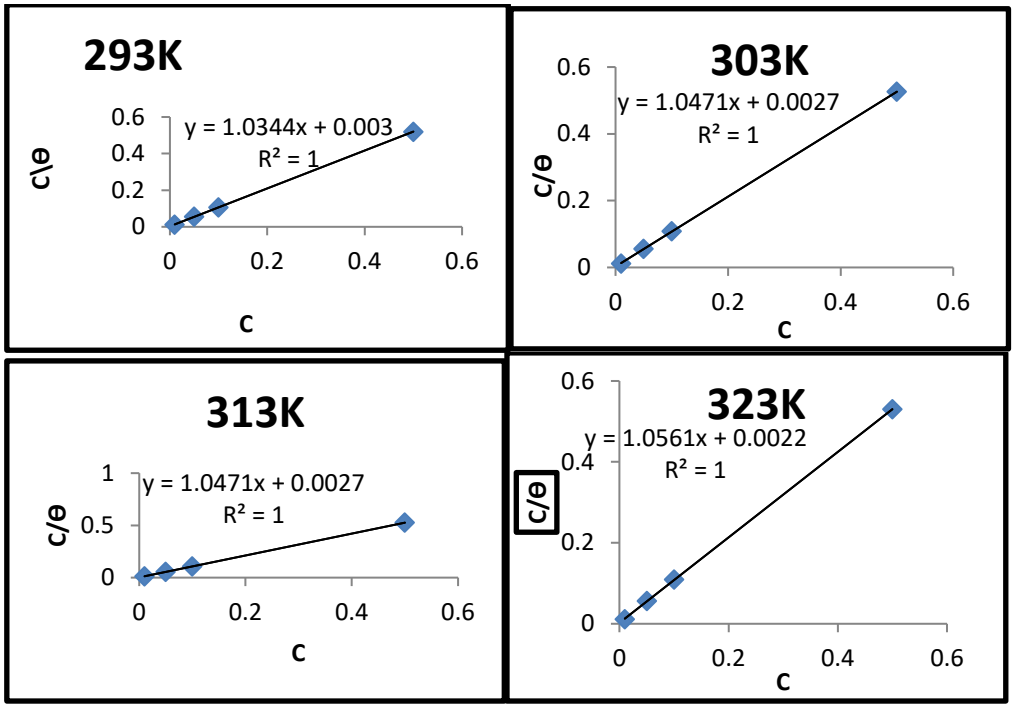

Figure 3: The Langmuir isotherm adsorption for carbon steel in 1M HCL at varied doses of inhibitor (Q1) at (293,303,313-323) Kelvin.

Table 7: The degree of surface coverage and the parameter of the adsorption isotherm for carbon steel in 1M HCL solution at varying doses of inhibitor (Q1) at (293,303,313 and 323) K.

T(K)	1/T(K^{-1})	C(M)	Ɵ	C/ Ɵ	K_{ads}(M^{-1})	r^2
293	0.00341	0.01	0.85	0.0117	333.33	1
		0.05	0.89	0.0561		
		0.1	0.93	0.1075		
		0.5	0.96	0.520		
303	0.00330	0.01	0.85	0.0117	500	1
		0.05	0.89	0.0561		
		0.1	0.92	0.108		
		0.5	0.95	0.526		
313	0.00319	0.01	0.85	0.0117	500	1
		0.05	0.89	0.0561		
		0.1	0.92	0.108		
		0.5	0.95	0.526		
323	0.00309	0.01	0.85	0.0117	500	1
		0.05	0.88	0.0568		
		0.1	0.91	0.109		
		0.5	0.94	0.531		

The effectiveness of this approach is evidenced by the strong correlation (r2) observed in the Langmuir adsorption isotherm. The equilibrium constant (Kads) for the adsorption-desorption process of the inhibitor can be determined from the reciprocal of the intercept. Table (7) presents the values of the adsorptive equilibrium constant (Kads) obtained from the data. Furthermore, the data in Table (7) demonstrate a slight increase in the adsorptive equilibrium constant (Kads) within the temperature range of (293, 303, 313, and 323) K.

3.7 Thermodynamic adsorption parameters

The adsorption free energy (ΔG_{ads}) is established by applying the following formula to the results obtained at various temperatures [39].

$$\Delta G_{ads} = -2.303\ RT \log (55.5\ K_{ads}) \quad \text{---------- 7}$$

A gas constant is (R), T is the temperature's absolute value. The water concentration is 55.5, Kads, the equilibrium constant for the inhibitor adsorption method data in Table (8) showed Values of ΔG_{ads}. The obtained values demonstrate a negative ΔGads, indicating favorable and efficient adsorption at the interface. Typically, ΔGads values equal to or lower than -23,939 K J mol-1 are indicative of electrostatic interactions between charged molecules and charged metal surfaces. Values significantly below this threshold suggest charge participation or transition from the inhibitor molecules to the metal surface, resulting in the formation of specific bonds (chemisorption). Based on the calculated ΔG(ads) values, it can be concluded that the tested inhibitor undergoes chemical adsorption onto the metal surface in the 1M HCl solution. Analyzing the graph of log Kads vs. 1/T, the adsorption heat (ΔHads) can be derived from the slope of the linear portion of the curve. ΔHads is approximately equal to -ΔHads/2.303R due to the constant pressure. In this case, the synthetic inhibitor exhibits a ΔHads value of 23.409 kJ mol-1, indicating an endothermic adsorption process. The positive value of ΔHads suggests chemisorption, while exothermic processes (ΔHads < 0) may result from physisorption, chemisorption, or a combination of both [38]. The magnitude of ΔHads can be utilized to distinguish between physisorption and chemisorption in exothermic processes. Physisorption typically has a ΔHads of less than 40 kJ mol-1, while chemisorption approaches 100 kJ mol-1. The equation below is employed to determine the entropy of inhibitor adsorption (ΔSads).

$$\Delta G_{ads} = \Delta H_{ads} - T\Delta S_{ads} \quad \text{……..(8).}$$

The Table (9) lists the values for ΔS_{ads} . It is noted that "ΔS_{ads} values" are positive in the presence of the inhibitor, indicating that an increase in disorder is caused by the adsorption of just one inhibitor molecule by the desorption of additional water molecules

Table 8: Data of degree of surface coverage and the parameter of adsorption isotherm for the adsorption inhibitor Q1 on carbon steel in 1M HCl solution

T K	1/T K^{-1}	Kads	Log K_{ads}	1000/T	ΔG_{ads} J.mol^{-1}.K^{-1}
293	0.00341	333.33	2.5228	3.412	-23,939
303	0.00330	500	2.6989	3.3003	-25,776
313	0.00319	500	2.6989	3.1948	-26,627
323	0.00309	500	2.6989	3.095	-27,477

Table 9: Thermodynamic information for the adsorption inhibitor Q1 on carbon steel in 1M HCl solution

T (K)	ΔG_{ads} k J.mol^{-1}.K^{-1}	ΔH_{ads} kJ.mol^{-1}.	ΔS_{ads} kJ.mol^{-1}.K^{-1}
293	-23,939	23.409	65.313
303	-25,776		62.577
313	-26,627		60.578
323	-27,477		58.702

3.8 Temperature effect

The correlation between corrosion rate and temperature was examined in a 1M HCl solution with and without inhibitors at varying concentrations (0.01M, 0.05M, 0.1M, and 0.5M). The influence of potentiostatic polarization on the temperature was taken into account for evaluating the apparent activation energy. Various electrochemical parameters were determined and presented in Table (7). It was observed that as the temperature increased, the corrosion current density (Icorr) also increased, while the inhibition efficiency (%IE) decreased. This behavior can be attributed to the interaction of inhibitors with the carbon steel

surface. At lower temperatures, physical adsorption predominated, while at higher temperatures, chemisorption became more favorable.

3.9 Parameters for activation

Also with thermodynamics, a kinetic model is used to explain how corrosion is inhibited. The corrosion reaction is described by Arrhenius equation [40].

$$\text{Log Icorr} = \log A - Ea^*/2.303RT \quad \text{.....[9]}$$

In the context of corrosion analysis, the corrosion current density (icorr) is denoted as the measure of the current flow, while the gas constant (R) represents a fundamental constant in thermodynamics. The energy of activation for the corrosion reaction (Ea*) and the absolute temperature (T) are key factors in understanding the corrosion process. Additionally, the Arrhenius pre-exponential factor (A) is used to quantify the relationship between the rate of reaction and temperature. Arrhenius graphs showing the relationship between the natural logarithm of the current density and 1/T, for a 1M solution of HCl, are shown in Figure (4) both with and without the presence of (0.01M ,0.05M ,0.1M and0.5M) at different temperatures. Equation (9) describes this relationship. In this study, a high value of Ea* indicates a reduced corrosion rate. Notably, the Ea* value is particularly high at 0.5M inhibitor concentration, leading to a significant reduction in the corrosion of the carbon steel surface [41-42]

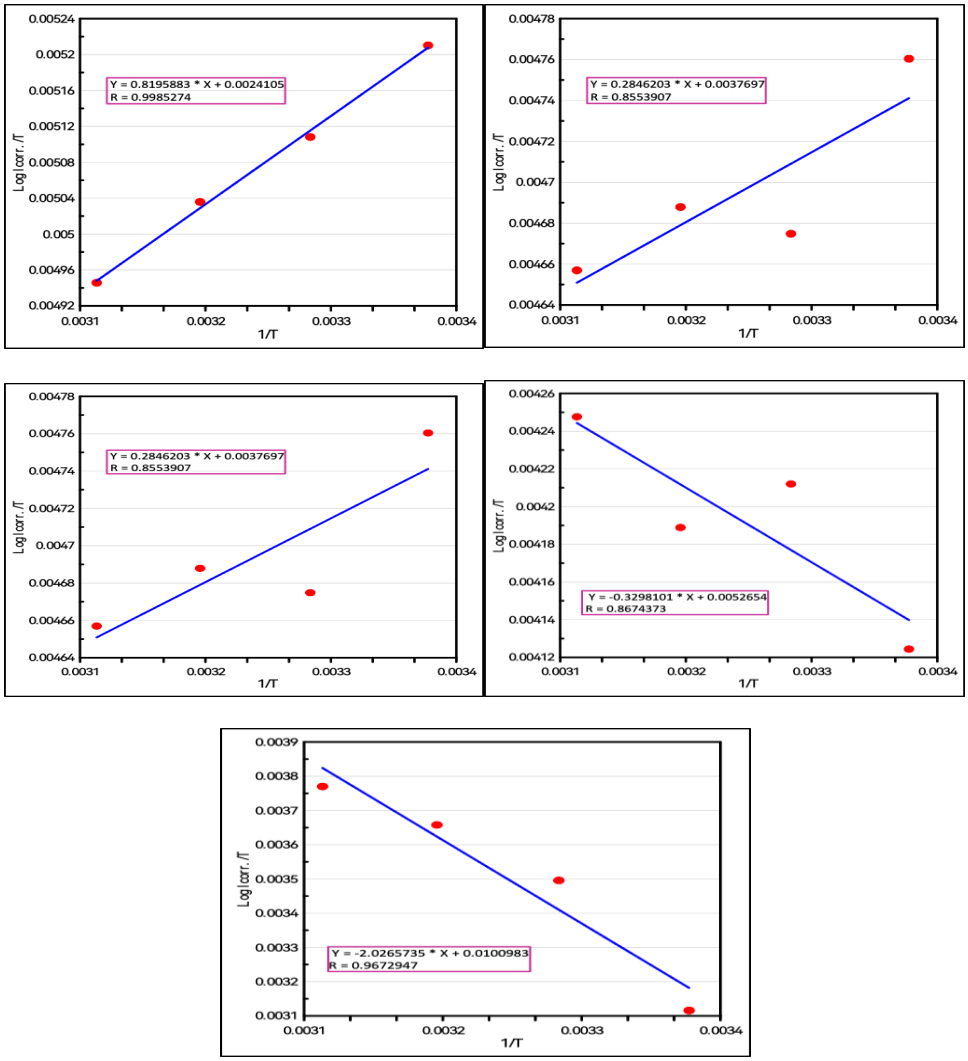

Figure 4: Arrhenius plots of log icorr/T against 1/T in the presence and absence of derivatives at concentrations of 0.01M, 0.05M, 0.1M, and 0.5M, measured at a range of temperatures.

The transition state equation (10) is used to compute the activation's enthalpy and entropy, (ΔH*and ΔS*)[43].

$$\text{Log Icorr / T} = (\log R/N\ Ah) + (\Delta S^*/2.303R) - (\Delta H^*/2.303RT) \quad \ldots\ldots\ldots\ldots(10)$$

R = universal gas constant ΔH*= activation enthalpy ΔS*= Activation entropy .
h =Planck's constant NA = Avogadro's number

Log (icorr/T) plotted versus 1/T (Eq. (10)), for a 1M solution of HCl, both with and without the presence of (0.01M ,0.05M ,0.1M and0.5M) at different temperatures, are shown in Figure (4) The values of ΔH*enthalpy and ΔS* entropy computed from the slope ((-ΔH*/ 2.303R)) and the intercept [log (R/NAh) + ΔS*/2.303R] of the straight lines are shown in Table (10).

Table 10: The thermodynamic characteristics activation of the synthetic inhibitor Q1 in 1M HCl

Sample	T(K)	ΔE* KJ/mol	ΔH* KJ/mol	ΔS* J/mol.K	ΔG* J/mol.K
BLANK	293	4.404598	-0.03151	-0.19757353	57.858
	303				59.833
	313				61.809
	323				63.785
0.01	293	4.365616	-0.01569	-0.19757385	57.873
	303				59.849
	313				61.825
	323				63.801
0.05	293	6.845523	-0.00545	-0.19754782	57.876
	303				59.852
	313				61.827
	323				63.802
0.1	293	9.52582	0.006315	-0.19751918	57.879
	303				59.855
	313				61.83
	323				63.805
0.5	293	18.19981	0.038803	-0.19742665	57.885
	303				59.859
	313				61.833
	323				63.808

Conclusions

The effectiveness of Schiff base derivatives in inhibiting corrosion was studied using a method that measures weight loss. In summary, the study revealed the effectiveness of various Schiff base derivatives as inhibitors for corrosion protection of carbon steel in a 1M HCl solution. Q1 emerged as the most potent inhibitor, followed by Q3, Q4, Q5, Q2. Increasing the inhibitor concentration enhanced the inhibition efficiency, with higher concentrations yielding greater effectiveness. The study found that increased temperature impaired the inhibitory capabilities of the derivatives, with corrosion protection diminishing at higher thermal conditions. The adsorption of Q1 onto the steel surface followed the Langmuir adsorption isotherm model, forming a protective layer. The results supported the notion of chemical bonding between the inhibitor and the metal surface, highlighting the strong interaction between them and their role in corrosion inhibition.

References

[1] Y. G. Avdeev, Y. I. Kuznetsov, and A. K. Buryak, "Inhibition of steel corrosion by unsaturated aldehydes in solutions of mineral acids", *Corrosion Science, 69, 50–60,* 2013.

[2] A. A. Al-Amiery, A. A. Kadhum, H. Mohamad, and S. Junaedi, "A novel hydrazinecarbothioamide as a potential corrosion inhibitor for mild steel in HCl", *Materials*, *6*(4), 1420-1431, 2013.

[3] M. A. Deyab, "Effect of cationic surfactant and inorganic anions on the electrochemical behavior of carbon steel in formation water", *Corrosion Science*, *49*(5), 2315-2328, 2007.

[4] D. Özkır, K. Kayakırılmaz, E. Bayol, A. Gürten, and F. Kandemirli, "The inhibition effect of Azure A on mild steel in 1 M HCl. A complete study: Adsorption, temperature, duration and quantum chemical aspects", *Corrosion Science*, *56*, 143-152, 2012.

[5] L. Fragoza-Mar, O. Olivares-Xometl, M. A. Domínguez-Aguilar, E. A. Flores, P. Arellanes-Lozada, and F. Jiménez-Cruz, "Corrosion inhibitor activity of 1, 3-diketone malonates for mild steel in aqueous hydrochloric acid solution", *Corrosion Science*, *61*, 171-184, 2012.

[6] M. A. Hegazy, A. S. El-Tabei, A. H. Bedair, and M. A Sadeq, "An investigation of three novel nonionic surfactants as corrosion inhibitor for carbon steel in 0.5 M H_2SO_4", *Corrosion Science*, *54*, 219-230, 2012.

[7] A. Khadiri, R. Saddik, K. Bekkouche, A. Aouniti, B. Hammouti, N. Benchat, and R. Solmaz, "Gravimetric, electrochemical and quantum chemical studies of some pyridazine derivatives as corrosion inhibitors for mild steel in 1 M HCl solution", *Journal of the Taiwan Institute of Chemical Engineers*, 58, 552-564, 2016.

[8] N. Hossain, M. A. Chowdhury, M. Rana, M. Hassan, and S. Islam, "Terminalia arjuna leaves extract as green corrosion inhibitor for mild steel in HCl solution", *Results in Engineering,* 100438,2022.

[9] A. A. Ayoola, R. Babalola, B. M. Durodola, E. E. Alagbe, O. Agboola, and E. O. Adegbile, "Corrosion inhibition of A36 mild steel in 0.5 M acid medium using waste citrus limonum peels", *Results in Engineering*, *15*, 100490. 2022.

[10] A. S. Jasim, K. H. Rashid, K. F. AL-Azawi, and A. A. Khadom, "Synthesis of a novel pyrazole heterocyclic derivative as corrosion inhibitor for low-carbon steel in 1M HCl: Characterization, gravimetrical, electrochemical, mathematical, and quantum chemical investigations", *Results in Engineering*, *15*, 100573, 2022.

[11] B. Tan, B. Xiang, S. Zhang, Y. Qiang, S. Chen, and J. He, "Papaya leaves extract as a novel eco-friendly corrosion inhibitor for Cu in H2SO4 medium", *Journal of Colloid and Interface Science*, 582, 918-931, 2021.

[12] O.H.R. Al-Jeilawi, H.N. Al-Ani, A. Al-Zahra and K.T.A. AL-Sultani,"Exploring the Potential of Quantum Chemical Calculations for Synthesized Quinazoline Derivatives as Superior Corrosion Inhibitors in Acidic Environment ", *Phys. Chem. Res.*, 12 (1), 205-217, 2024.

[13] A. K. Singh, and M. A. Quraishi, "Study of some bidentate Schiff bases of isatin as corrosion inhibitors for mild steel in hydrochloric acid solution", *International Journal of Electrochemical Science*, *7*(4), 3222-3241, 2012.

[14] A. Q. Oleiwi, O. H. Al-Jeilawi, and S. A. Dayl, "Synthesis, Characterization of Some Thiourea Derivatives Based on 4-Methoxybenzoyl Chloride as Antioxidants and Study of Molecular Docking", *Iraqi Journal of Science*, 64(1), 1-12, 2023.

[15] A. M. Nassar, A. M. Hassan, and M. A. Shoeib, "Synthesis, characterization and anticorrosion studies of new homobimetallic Co (II), Ni (II), Cu (II), and Zn (II) Schiff base complexes", *Journal of Bio-and Tribo-Corrosion*, *1*(3), 1-16, 2015.

[16] A. Singh, K. R. Ansari, D. S. Chauhan, M. A. Quraishi, H. Lgaz, and I. M. Chung, "Comprehensive investigation of steel corrosion inhibition at macro/micro level by ecofriendly green corrosion inhibitor in 15% HCl medium", *Journal of colloid and interface science*, 560, 225-236, 2020.

[17] N. M. Hashim, A. A. Rahim, H. Osman, and P. B. Raja, "Quinazolinone compounds as corrosion inhibitors for mild steel in sulfuric acid medium", *Chemical Engineering Communications*, *199*(6), 751-766, 2012.

[18] G. G ASTM, "standard practice for laboratory immersion corrosion testing of metals", *West Conshohocken*, PA, 31-72, 1990.

[19] H. El-Kashef, A. R. Farghaly, A. Al-Hazmi, T. Terme, and P. Vanelle, "Pyridine-based heterocycles. Synthesis of new pyrido [4', 3': 4, 5] thieno [2, 3-d] pyrimidines and related heterocycles", *Molecules*, *15*(4), 2651-2666, 2010.

[20] R. R. Nasab, M. Mansourian, and F. Hassanzadeh, "Synthesis, antimicrobial evaluation and docking studies of some novel quinazolinone Schiff base derivatives", *Research in Pharmaceutical Sciences*, *13*(3), 213, 2018.

[21] M. Ajmal, A. S. Mideen, and M. A. Quraishi, "2-hydrazino-6-methyl-benzothiazole as an effective inhibitor for the corrosion of mild steel in acidic solutions", *Corrosion science*, *36*(1), 79-84, 1994.

[22] M. Scendo, and M. Hepel, "Inhibiting properties of benzimidazole films for Cu (II)/Cu (I) reduction in chloride media studied by RDE and EQCN techniques", *Journal of Electroanalytical Chemistry*, *613*(1), 35-50, 2008.

[23] R. Kareem, and M. S. Shihab, "Synthesis New Pyridinium Salts as Corrosion Inhibitors for Mild Steel in 1 M H_2SO_4", *Al-Nahrain Journal of Science*, *24*(2), 14-20, 2021.

[24] O. H. Al-Jeilawi, and N. A. Khudhair, "Novel Synthesis of Some N-Hydroxy Phthalimide Derivatives with Investigation of Its Corrosion Inhibition for Carbon Steel in HCl Solution", *Chemical Methodologies*, *5*(4), 331-340, 2020.

[25] L. Latheef, and M. P. Kurup, "synthesis and spectral studies of 3-azacyclothiosemicarbazones", *Journal of Advanced Scientific Research*, 10(04 Suppl 2), 333-338, 2019.

[26] N. S. Turkey, J. N. Jeber, "Turbidimetric Determination of Mebeverine Hydrochloride in Pharmaceutical Formulations Using Two Consecutive Detection Zones under Continuous Flow Conditions", Baghdad Science Journal, 16(4), 600 - 613, 2022.

[27] R.M. Sliverstien, F. X. Websters, and D.J. Kiemle, "Spectrometric identification of organic compounds*"*. 7th Edition. John Wiely and Sons. New York.2005.

[28] O.H. Al-Jeilawi and, M.A. Al-Yassiri, "Synthesis, Characterization and Quantum Mechanical Study of Some New 2-benzylidenehydrazinecarbothioamide Derivatives as Corrosion Inhibitors for Carbon/mild Steel in Acidic Medium", *Iraqi Journal of Science*, *56*(1A), 1-11, 2015.

[29] S. Issaadi, T. Douadi, A. Zouaoui, S. Chafaa, M.A. Khan, and G. Bouet, "Corrosion inhibition of mild steel by two new S-heterocyclic compounds in 1 M HCl: experimental and computational study", *Corros. Sci.*, *53*, 1484, 2011.

[30] M. Scendo, and M. Hepel, "Inhibiting properties of benzimidazole films for Cu (II)/Cu (I) reduction in chloride media studied by RDE and EQCN techniques", *Journal of Electroanalytical Chemistry*, *613*(1), 35-50, 2008.

[31] M. Scendo, "Corrosion inhibition of copper by purine or adenine in sulphate solutions", *Corrosion Science*, *49*(10), 3953-3968, 2007.

[32] Z.T. Khudhair, and M.S. Shihab, "Study of synergistic effect of some pyrazole derivatives as corrosion inhibitors for mild steel in 1 M H_2SO_4", *Surface Engineering and Applied Electrochemistry*, 56(5), 601-609, 2020.

[33] O. H. Al-Jeilawi, "Corrosion Inhibition for Carbon Steel of Benzimidazole Derivatives Synthesized in Sulfuric Acid Solution", *International journal of science and research*, 6, 78-96, 2017.

[34] S. M. Al-Majidi, U. H. Al-Jeilawi, and A. S. Khulood, "Synthesis and characterization of some 2-sulphanyl benzimidazole derivatives and study of effect as corrosion inhibitors for carbon steel in sulfuric acid solution", *Iraqi Journal of Science*, *54*(4),789-802, 2013.

[35] N. Labjar, M. Lebrini, F. Bentiss, N. Chihib, S. El Hajjaji, and C. Jama, "Corrosion inhibition of carbon steel and antibacterial properties of aminotris-(methylenephosphonic) acid", *Mater. Chem. Phys.*, 119, 330-336, 2010.

[36] A. Al-Zahra, H. N. Al-Ani, & O. H. Al-jeilawi, "Experimental and Theoretical Study Of 3-Benzyl-2-Mercaptoquinoizoline-4 (3h)-One (Bmq) As An Inhibitor Of Carbon Steel Corrosion In Acidic Media", International Journal of Science and Nature,9,105-113,2018.

[37] A. Kosari, M. Momeni, R. Parvizi, M. Zakeri, M. H. Moayed, A. Davoodi, and H. Eshghi, "Theoretical and electrochemical assessment of inhibitive behavior of some thiophenol derivatives on mild steel in HCl", *Corrosion science*, 53, 3058–3067, 2011.

[38] M. Abdallah, "Rhodanine azosulpha drugs as corrosion inhibitors for corrosion of 304 stainless steel in hydrochloric acid solution", *Corrosion Science.*, 44 ,717–728,2001.

[39] F. S. Abd, and A. H. Ali, "Egy-dronate drug as promising corrosion inhibitor of C-steel in aqueous medium", *Zaštita materijala*, *59*(1), 126-140, 2018.

[40] O. Benali, L. Larabi, S. Merah, and Y. Harek, "Influence of the Methylene Blue Dye (MBD) on the corrosion inhibition of mild steel in 0.5 M sulphuric acid, Part I: weight loss and electrochemical studies", *J. Mater. Environ. Sci*, *2*(1), 39-48, 2011.

[41] A. K. Singh, and M. A. Quraishi, "Investigation of adsorption of isoniazid derivatives at mild steel/hydrochloric acid interface: Electrochemical and weight loss methods", *Materials Chemistry and Physics*, *123*(2-3), 666-677,2010.

[42] N. S. Turkey, J. N. Jeber, "Flow Injection Analysis with Turbidity Detection for the Quantitative Determination of Mebeverine Hydrochloride in Pharmaceutical Formulations", *Baghdad Science Journal*, 19(1), 0141, 2022.

[43] U. H. Al-Jeilawi, S. M. Al-Majidi, and K. A. Al-Saadie, "Corrosion Inhibition Effects of Some New Synthesized N-Aroyl-N-Aryl thiourea Derivatives for Carbon Steel in Sulfuric Acid Media", *Al-Nahrain Journal of Science*, *16*(4), 80-93, 2013.